Development 137, 405-415 (2010) doi:10.1242/dev.045369

Pax6-dependent *Shroom3* expression regulates apical constriction during lens placode invagination

Timothy F. Plageman, Jr[1,2], Mei-I Chung[3], Ming Lou[4], April N. Smith[1,2], Jeffrey D. Hildebrand[5], John B. Wallingford[3,6] and Richard A. Lang[1,2,7,8,*]

SUMMARY

Embryonic development requires a complex series of relative cellular movements and shape changes that are generally referred to as morphogenesis. Although some of the mechanisms underlying morphogenesis have been identified, the process is still poorly understood. Here, we address mechanisms of epithelial morphogenesis using the vertebrate lens as a model system. We show that the apical constriction of lens epithelial cells that accompanies invagination of the lens placode is dependent on Shroom3, a molecule previously associated with apical constriction during morphogenesis of the neural plate. We show that Shroom3 is required for the apical localization of F-actin and myosin II, both crucial components of the contractile complexes required for apical constriction, and for the apical localization of Vasp, a Mena family protein with F-actin anti-capping function that is also required for morphogenesis. Finally, we show that the expression of Shroom3 is dependent on the crucial lens-induction transcription factor Pax6. This provides a previously missing link between lens-induction pathways and the morphogenesis machinery and partly explains the absence of lens morphogenesis in Pax6-deficient mutants.

KEY WORDS: Mena (Enah), Pax6, Shroom3, Vasp, Lens, Morphogenesis, Mouse, Chicken, *Xenopus*

INTRODUCTION

Embryonic development requires complex events in morphogenesis that are driven by changes in cell shape, migration, proliferation and death. Although progress has been made in understanding some of the mechanisms underlying morphogenesis (Lecuit and Lenne, 2007), our knowledge is still limited. During early development of the ocular lens, a region of surface ectoderm adjacent to the optic vesicle thickens to form the lens placode. This placode then invaginates in coordination with the presumptive retina and forms the lens pit and optic cup. This relatively simple morphogenesis event serves as a useful model with which to study the mechanisms involved.

There is a strong case that the genes required for fate decisions during induction of the lens placode are closely linked to the morphogenesis machinery. For example, mice mutant for *Pax6* (Grindley et al., 1995; Ashery-Padan et al., 2000; Smith et al., 2009), *Bmp7* (Wawersik et al., 1999) or the Fgf receptor adaptor *Frs2α* (Gotoh et al., 2004) all show failure of lens fate acquisition coupled to a failure of morphogenesis. Although the phenotype of the *Bmp7* and *Frs2α*^{2F} mutants is variable (Wawersik et al., 1999; Gotoh et al., 2004), either germline or presumptive lens conditional mutation of *Pax6* gives a very consistent failure of lens placode invagination (Grindley et al., 1995; Ashery-Padan et al., 2000; Smith et al., 2009) that contrasts, for example, with lens placode conditional deletion of *Sox2*, in which invagination is still initiated (Smith et al., 2009). These observations raise the possibility of identifying components of the morphogenesis machinery that provide the crucial links to inductive pathways.

The individual epithelial cells within the prospective lens pit undergo a cell shape change from cylindrical to conical during invagination, in which the apical circumference of the cell is reduced (Hendrix and Zwaan, 1974). This shape change, known generally as apical constriction (AC), is a characteristic shared with the prospective mesodermal cells of a gastrulating *Drosophila* embryo, as well as with the neuroepithelial cells that contribute to the hinge-point region during neural tube closure (Lecuit and Lenne, 2007). The driving force behind AC is the activation of apical non-muscle myosins (Dawes-Hoang et al., 2005), which induce contraction of actin-myosin complexes and reduce the apical area. Analysis of *Drosophila* gastrulation has determined that non-muscle myosin activation during AC is triggered by Rho kinase (Rok), which is activated and apically concentrated by RhoGEF2 and Rho1 (Barrett et al., 1997; Hacker and Perrimon, 1998; Nikolaidou and Barrett, 2004; Dawes-Hoang et al., 2005; Kolsch et al., 2007). In vertebrate morphogenesis, the requirement for non-muscle myosin-driven AC has been demonstrated (Haigo et al., 2003; Hildebrand, 2005; Lee and Harland, 2007); however, the mechanisms that regulate its activity are less well defined than in *Drosophila*.

A potent inducer of AC in vertebrates is the cytoskeletal protein Shroom3. Shroom3 is an actin-binding protein that is both necessary and sufficient to induce AC during neural tube closure in frogs and mice (Haigo et al., 2003; Hildebrand, 2005; Lee et al., 2007). Shroom3 loss-of-function in frogs and mice results in the accumulation of F-actin at the base of the cell and a failure of AC (Hildebrand and Soriano, 1999; Haigo et al., 2003). Shroom3 AC activity, which is both Rho kinase- and non-muscle myosin-dependent, has been mapped to the ASD2 domain of Shroom3, a region that also binds and recruits the Rho kinases Rock1 and Rock2 (Hildebrand, 2005;

[1]The Visual Systems Group, [2]Divisions of Pediatric Ophthalmology and [7]Developmental Biology, Children's Hospital Research Foundation, Cincinnati Children's Hospital Medical Center, 3333 Burnet Avenue, Cincinnati, OH 45229-3039, USA. [3]Molecular, Cell and Developmental Biology, University of Texas at Austin, Austin, TX 78712, USA. [4]Department of Chemistry and Physics, Lamar University, Beaumont, TX 77710, USA. [5]Department of Biological Sciences, University of Pittsburgh, Pittsburgh, PA 15260, USA. [6]Howard Hughes Medical Institute, 4000 Jones Bridge Road, Chevy Chase, MD 20815-6789, USA. [8]Department of Ophthalmology, University of Cincinnati, Cincinnati, OH 45229, USA.

*Author for correspondence (Richard.Lang@cchmc.org)

Accepted 3 December 2009

Nishimura and Takeichi, 2008). Although this domain is found in all members of the Shroom protein family (Shroom1-4), only Shroom3 is capable of inducing AC (Dietz et al., 2006). Other shared domains in this family include a PDZ domain, which is dispensable for AC, and the ASD1 domain, an actin-binding region implicated in cellular localization of Shroom3 (Haigo et al., 2003; Hildebrand, 2005; Dietz et al., 2006). Although its function has not been investigated, Shroom3 also possesses a proline-rich sequence (FPPPP or FPn) that matches the consensus binding site of the EVH1 domain-containing proteins (Hildebrand and Soriano, 1999; Ball et al., 2002). It is presumed that another domain within Shroom3 is also required for its AC function because the ASD2 domains from other Shroom proteins can induce AC when fused to a large region containing the ASD1 and proline-rich domains of Shroom3 (Dietz et al., 2006). Further analysis of the Shroom3 domains is necessary to understand the mechanisms of Shroom3 function.

Members of the Mena/Vasp family of proteins are also implicated in vertebrate AC (Roffers-Agarwal et al., 2008). This family, which comprises vertebrate homologs of the *Drosophila* protein Enabled (Ena), is involved in many examples of actin dynamics, including the assembly of actin filament networks (Krause et al., 2003). In *Drosophila*, morphogenesis of epithelial tissues is disrupted and, as for *Shroom3* mutants, the accumulation of apical actin is lost in *ena* mutants (Baum and Perrimon, 2001; Gates et al., 2007; Gates et al., 2009). Xena, the *Xenopus* homolog of Ena, is apically enriched in the neural plate and is required for neuroepithelial AC, neural tube closure and apical actin enrichment (Roffers-Agarwal et al., 2008). Similarly, gene-targeted mice with different allelic combinations of its three Ena homologs, Mena (Enah – Mouse Genome Informatics), Vasp and Evl, also have neural tube closure defects and mislocalization of actin in the neuroepithelium (Menzies et al., 2004; Kwiatkowski et al., 2007). These data are consistent with a role for Mena/Vasp proteins in facilitating the localized apical assembly of actin filaments in epithelia undergoing AC. Interestingly, the Mena/Vasp proteins, via their EVH1 domain, bind to proteins that contain the proline-rich consensus found in many actin-associated cytoskeletal proteins (Hildebrand and Soriano, 1999; Ball et al., 2002). Currently, it is not known how Ena/Vasp proteins are apically localized during vertebrate AC.

In the present study, we utilized a mutant gene-trapped mouse line with a disruption in *Shroom3* [the *Shroom3*$^{Gt/Gt}$ allele (Hildebrand and Soriano, 1999)] to determine whether it is required for lens pit cell AC. Cell shape analysis revealed that the cells within the lens pit of these mutants fail to fully apically constrict, resulting in smaller and misshapen lens pits. Mutant lens pits also displayed a redistribution of F-actin, similar to what is observed with Shroom3 and Ena/Vasp loss-of-function mutations (Hildebrand and Soriano, 1999; Haigo et al., 2003; Menzies et al., 2004; Roffers-Agarwal et al., 2008). Because of the similarity in phenotypes and the potential for Shroom3 and Ena/Vasp proteins to interact, the function of the proline-rich EVH1-binding domain was examined. We showed that this domain is essential for Shroom3-mediated AC and apical Vasp recruitment. It was also determined that Shroom3 expression in the prospective lens is dependent on Pax6, thus defining a link between inductive signaling and the morphogenesis machinery. Together, these data provide novel insights into mechanisms of epithelial morphogenesis and, more specifically, of lens pit invagination.

MATERIALS AND METHODS

Animal maintenance and use

Mice were housed in a specific pathogen-free vivarium in accordance with institutional policies. A gestational age of 0.5 days was defined as the day of detection of a vaginal plug [embryonic day (E) 0.5]. At specific gestational ages, fetuses were removed by hysterectomy after the dams had been anesthetized with isoflurane. *Shroom3*$^{Gt/Gt}$ mice [in full, *Shroom3*$^{Gt(ROSA)53Sor}$] have been described previously (Hildebrand and Soriano, 1999).

Electroporation

Chicken embryos were obtained from standard pathogen-free (SPF) fertilized chicken eggs (Charles River Laboratories) following incubation in a humid environment at 37.5°C for ~45 hours (stage 11). Live embryos were removed via filter paper rings centered around the embryo and placed on a bed of thick albumin and overlaid with M199 media (Mediatech) supplied with 1% Penn/Strep (Mediatech). Exogenous expression was achieved by first mixing plasmid DNA (1-3 mg/ml) with particles of Fast Green FCF (Sigma, F7252) to visualize the DNA solution, pipetting the DNA using a pulled glass needle and mouth pipette (Sigma, A5177) into the space immediately adjacent to the presumptive lens, placing an electrode (BTX, 45-0116) on either side of the head and applying five 30-millisecond pulses (100 milliseconds between each pulse) of 20 volts using a BTX ECM 830 electroporator. Embryos were returned to the incubator and analyzed 20-24 hours later.

Xenopus experiments

Ectopic lenses were induced by injecting *Pax6* mRNA into the animal pole of half the blastomeres of two- or four-cell embryos as described previously (Altmann et al., 1997; Chow et al., 1999). *Shroom3* in situ hybridization and animal cap assays were performed as previously described (Lee et al., 2009).

Immunofluorescence

Immunofluorescence (IF) labeling of cryosections was performed as described (Smith et al., 2005). The primary antibodies used were: anti-β-catenin (1:500, Santa Cruz, sc-7199), anti-ZO1 (1:500, Invitrogen, 61-7300), anti-myosin IIB (1:5000, Covance, PRB445P), anti-Pax6 (1:1000, Covance, PRB-278P), anti-Flag (1:500, Sigma, F1804), anti-V5 (1:500, Invitrogen, 46-0705) and anti-Vasp (1:1000, Cell Signaling, 3132). Alexa Fluor secondary antibodies were used at 1:1000 (Invitrogen, A10680, A-11012, A-11001, A-11019, A-21207). The Shroom3 (1:1000) and Vasp (1:1000) specific rabbit polyclonal antibodies used for staining cryosectioned embryos were generous gifts from Jeff Hildebrand (Hildebrand, 2005) and Frank Gertler (Menzies et al., 2004), respectively. Phalloidin (Invitrogen, A12381, A12379) staining to visualize F-actin was at 1:1000. For visualization of nuclei, sections were counterstained with Hoechst 33342 (Sigma, B-2261). Whole embryo staining was performed in the same manner as for the cryosections.

Immunofluorescence quantification

Apical/basal ratios of phalloidin and myosin II staining were calculated from drawing a line along the apical and basal membranes of stained 10 μm cryosections using ImageJ v1.33 (NIH). The signal intensity of every pixel along the drawn line was tabulated and averaged and expressed as a ratio for each lens pit. The ratios for at least 11 lens pits were averaged. The IF intensity along the apical/basal axis for Shroom3-, phalloidin- and Vasp-stained cryosections was determined using ImageJ. The average IF profile was quantified by first normalizing to the average IF intensity of each image, normalizing to cell height, and calculating the average pixel intensity along the apical/basal axis for at least 25 cells from four or five lens pits. Statistical significance was determined by Student's *t*-test.

Shape/area quantification

Cell profiles were traced and compiled from images of phalloidin- and β-catenin-stained 10 μm cryosections using Photoshop CS4 (Adobe). Width measurements along the apical/basal axis and the height of every lens pit cell within a mid-pit cryosection from at least six different embryos of each genotype were taken using Axiovision (Zeiss). Only cells positive for the transgene in electroporated chicken lens pit cells were quantified. Apical area quantification was performed using images of phalloidin/ZO1-stained whole embryos, tracing the apical areas in Photoshop and using ImageJ v1.33 to measure the traced areas. Statistical significance was determined by Student's *t*-test. Analysis of lens pit curvature was performed as previously described (Chauhan et al., 2009).

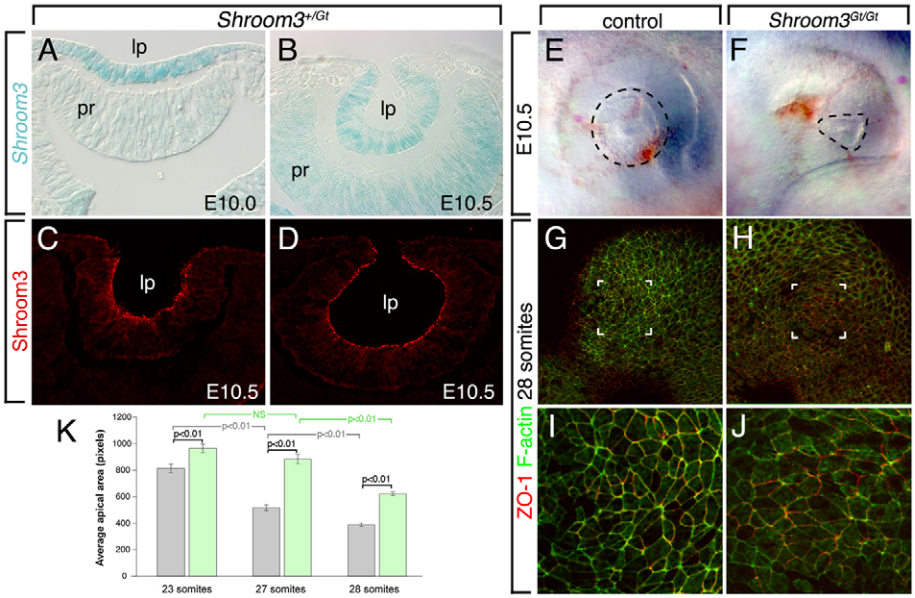

Fig. 1. Shroom3 is expressed in the invaginating lens pit and is required for apical constriction. (**A**,**B**) X-gal staining of cryosections through the lens pit of *Shroom3*$^{+/Gt}$ mouse embryos indicating expression of *Shroom3* mRNA. (**C**,**D**) Immunofluorescent staining of cryosections of wild-type embryos indicating Shroom3 protein localization. lp, lens pit; pr, presumptive retina. (**E**,**F**) Whole-mount view of the eye region of control (E) and *Shroom3* homozygous mutant (F) embryos. The lens pit is outlined (dashed line). (**G-J**) Surface view of 28-somite (~E10.0) control (G,I) or *Shroom3* homozygous mutant (H,J) lens placode immunofluorescently stained with a ZO1 antibody (red) and phalloidin (green) to identify apical junctions between cells. Lens pit invagination is first detectable at 28 somites. I and J are magnifications of the bracketed area in G and H, respectively. (**K**) Quantification of the apical area per cell for lens pit cells from control (gray) and *Shroom3*$^{Gt/Gt}$ (green) embryos that were somite-staged as indicated. One-way ANOVA analysis was performed to generate *P*-values and indicate statistical significance. NS, not significant.

DNA constructs/transfection

To generate Flag-tagged Shroom3 (Shroom3-Flag), the ~1500 bp *Eco*RI/*Not*I-digested fragment of pCS2-Shroom3 (generously provided by Jeff Hildebrand) was replaced with a PCR fragment [produced using the following primers (5′ to 3′): CAGAATTCCCAGGGTGATTGG, GATTACAAGGATGACGACGATAAGTAGTCGCCGGATCCTCTAGAACT and CTACTTATCGTCGTCATCCTTGTAATCAAGAGGAGAGGTCAACGTTG] that contained the same sequence plus the Flag tag sequence. Shroom3ΔFPn was generated by replacing a ~2100 bp *Age*I/*Not*I fragment from pCS2-Shroom3 with a PCR product generated from two rounds of PCR and primers that skipped over the consensus EVH1-binding site (GTGAATGGCACAGATCAAGCCCTGTGTGAG, CTCACACAGGGCTTGATCTGTGCCATTCAC, GTTACCGGTCACAGCTTGCC and CCGCGGCCGCGAATTAAAAAACCTC). The dominant-negative chicken Shroom3 (DN-cShroom3-V5) and dominant-negative mouse Mena (DN-Mena-V5) constructs were generated by inserting a PCR product, generated from chicken or mouse embryonic cDNA (SuperScript RT Kit, Invitrogen) and the primers CACCATGGGGAGGAGCCGGCTCAGCTCT and GTGGGATCGCTCCCTGAGCAG (DN-cShroom3-V5) or CACCATGAGTGAACAGAGTATCTGTC and TGAATTTAACACTTCTAAGGCA (DN-Mena-V5), in frame into the pcDNA3.1/V5-His-TOPO-V5 vector (Invitrogen). For transient transfections, MDCK cells were grown to ~30% confluency and transfected with 1 μg of plasmid DNA using Lipofectamine reagent as per the manufacturer's instructions (TransIT-293, Mirus).

RESULTS

Shroom3 is required for apical constriction during lens placode invagination

It has been established that invagination of the lens placode to form a lens pit is accompanied by a transition in epithelial cell shape from cylindrical to conical (Hendrix and Zwaan, 1975). Since Shroom3 is known to impose AC and thus a conical shape on epithelial cells (Haigo et al., 2003), it was an excellent candidate for involvement in lens pit invagination. To determine whether *Shroom3* is expressed during morphogenesis of the lens, we performed two analyses. First, as the mouse *Shroom3*^{Gt} locus splices *lacZ* into the *Shroom3* transcript, we could use X-gal staining as a reporter of *Shroom3* transcription. In E10.0 and E10.5 *Shroom3*$^{+/Gt}$ embryos stained with X-gal, reporter activity was observed prominently in the lens pit (Fig. 1A,B) and at a lower level in the presumptive retina at E10.5 (Fig. 1B). Immunofluorescence (IF) labeling showed that Shroom3 was localized at the apex of the epithelial cells that make up the lens pit (Fig. 1C,D).

Embryos mutant for *Shroom3* showed defects in lens morphogenesis and reduced AC. At E10.5, control embryos visualized in whole-mount showed a lens pit region that had invaginated (Fig. 1E). In *Shroom3*$^{Gt/Gt}$ embryos at E10.5, the region of the lens pit was smaller and of irregular shape (Fig. 1F). *Shroom3*$^{Gt/Gt}$ and control embryos at 23, 27 and 28 somites were labeled in whole-mount for F-actin and for the tight junction protein ZO1 (Tjp1 – Mouse Genome Informatics) to mark the apex of the lens pit cells. The lens placode or pit ectoderm was then visualized en face (Fig. 1G-J) and the apical areas of the cells measured (Fig. 1K). This showed, as expected, that the apical area was decreasing in control mice during this phase of invagination (Fig. 1K, gray bars), whereas *Shroom3*$^{Gt/Gt}$ embryos showed an increased apical area and thus reduced AC. These data showed that Shroom3 is required for AC in the lens.

It has been observed previously that in Shroom3-deficient cells, F-actin and myosin II complexes are reduced at the apex of the cell (Hildebrand and Soriano, 1999; Hildebrand, 2005). This has led to the suggestion that one function of Shroom3 is to direct actin-myosin contractile complexes to the cell apex, where they can

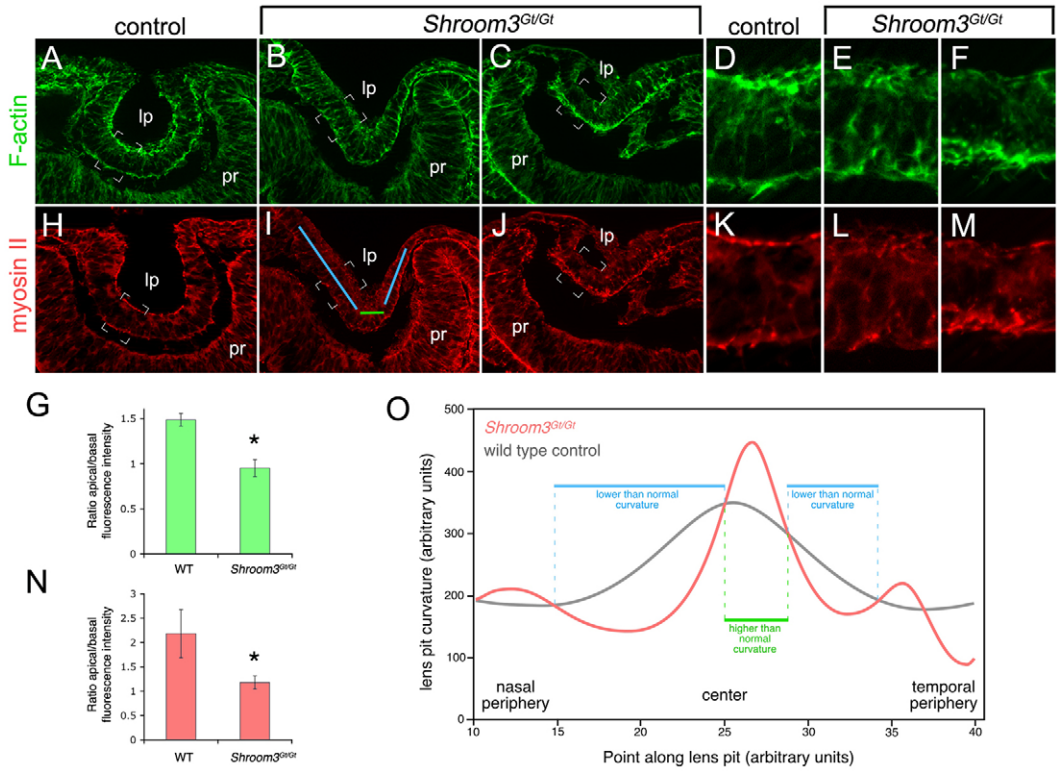

Fig. 2. F-actin and myosin II are mislocalized in the lens pits of *Shroom3* mutant embryos. (**A-F**,**H-M**) Cryosectioned E10.5 lens pits from control or *Shroom3*$^{Gt/Gt}$ mutant mice labeled with phalloidin to visualize F-actin (A-F) or with an antibody specific to myosin II (H-M). D-F and K-M are magnifications of the indicated regions of A-C and H-J, respectively. The blue and green lines in I refer to regions of distinct curvature in control and *Shroom3*$^{Gt/Gt}$ lens pit as quantified in O. lp, lens pit; pr, presumptive retina. (**G**,**N**) Quantification of F-actin (G) and myosin II (N) labeling intensity along the apical and basal surfaces of the lens pit in E10.5 control and *Shroom3*$^{Gt/Gt}$ embryos. *, $P<0.05$ by Student's *t*-test. (**O**) Quantification of rate of change of curvature along the basal surface of control (gray line) and *Shroom3*$^{Gt/Gt}$ (red line) lens pits. Regions where the mutant shows lower than normal curvature (blue lines) or higher than normal curvature (green line) are indicated.

mediate AC (Hildebrand and Soriano, 1999; Haigo et al., 2003; Hildebrand, 2005). In control embryos at E10.5, F-actin (Fig. 2A,D) in the lens pit epithelium was concentrated at both the apical and basal surfaces. The quantity of F-actin complex at the apex was higher, as indicated by an apical/basal quantification ratio of 1.5 (Fig. 2G). In *Shroom3*$^{Gt/Gt}$ embryos at E10.5, both mildly (Fig. 2B,E) and severely (Fig. 2C,F) affected embryos showed a change in the distribution of F-actin, in which the basal intensity appeared either equal to (Fig. 2B,E) or greater than (Fig. 2C,F) the apical intensity. Quantification confirmed this, with an apical/basal F-actin labeling ratio of 0.95 (Fig. 2G). A similar redistribution of myosin II was observed within the lens pit epithelial cells of *Shroom3*$^{Gt/Gt}$ embryos at E10.5 (Fig. 2H-N).

The overall shape of the lens pit in *Shroom3*$^{Gt/Gt}$ embryos was abnormal (for example, Fig. 2B), being V-shaped rather than of smooth curvature (Fig. 2A). The average change in lens pit shape among many embryos was documented using a quantitative analysis of curvature (Fig. 2O), as performed previously for other mutants (Chauhan et al., 2009). This showed that the *Shroom3*$^{Gt/Gt}$ lens pit has regions of low curvature (Fig. 2O, blue lines) that correspond to straight stretches of epithelium (Fig. 2I, blue lines) and that these straight stretches are separated by epithelial bends of very high curvature (Fig. 2O,I, green lines). We have recently shown that filopodia join the presumptive lens and retina and help coordinate invagination (Chauhan et al., 2009). These filopodia might provide an explanation for the lens pit invagination in the *Shroom3*$^{Gt/Gt}$ mutants in which the cylindrical-to-conical shape transition is defective (see Discussion). Regardless, reduced AC (Fig. 1) and increased basal actin and myosin II accumulation (Fig. 2) suggest that in the setting of the lens pit, the basic function of Shroom3 is likely to be similar to that previously documented (Hildebrand and Soriano, 1999; Haigo et al., 2003; Hildebrand, 2005).

The reduced apical area of the lens pit epithelial cells of *Shroom3* mutants (Fig. 1) suggested that we might detect changes in cell shape consistent with a failure to transition from cylindrically to conically shaped cells. To assess this, we labeled cryosections of control and *Shroom3*$^{Gt/Gt}$ lens pits for F-actin and β-catenin (Fig. 3A-D) so that cell borders were easily detected, and generated a series of cell shape profiles by manual tracing (Fig. 3E,F). The cell profiles were placed on a grid (Fig. 3E,F) and cell width and height measurements taken and presented graphically (Fig. 3G-I). This showed that, consistent with measurements of apical area (Fig. 1), lens pit cells in the *Shroom3* mutant had a significantly increased apical width (Fig. 3G,I). The *Shroom3* mutant lens cells did not differ from control cells with respect to basal width, but were significantly shorter (Fig. 3G,I). These changes are consistent with a function for Shroom3 in the elongation and apical constriction of cells (Haigo et al., 2003; Hildebrand, 2005; Lee et al., 2007).

Shroom3 is known to mediate AC and elongation in cells of the *Xenopus* neural plate (Haigo et al., 2003; Lee et al., 2007) and is likely to have a highly conserved function throughout the vertebrates

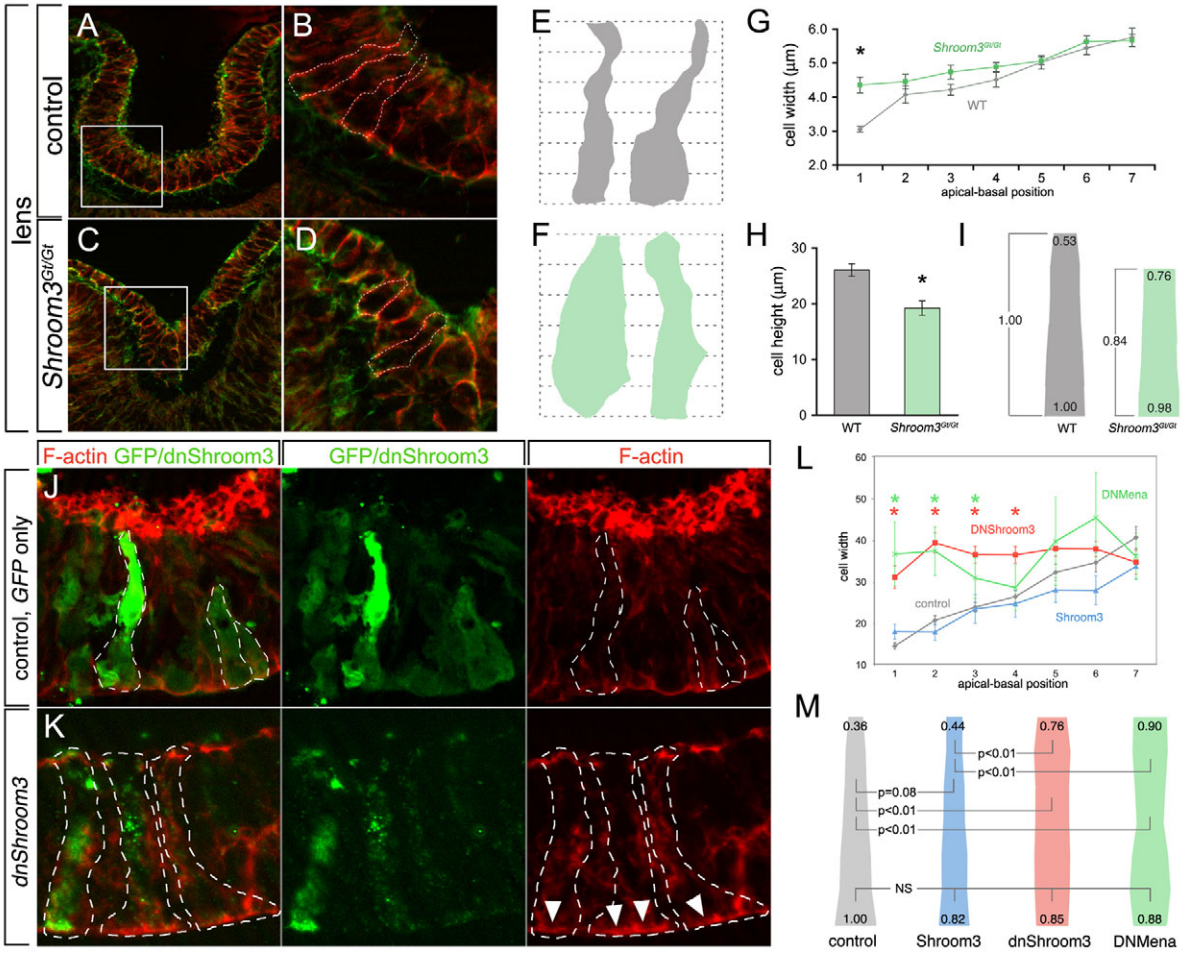

Fig. 3. Shroom3-deficient embryos have altered lens pit cell shapes. (**A-D**) Representative images of β-catenin (red) and phalloidin (green) labeled lens pit cryosections from control and *Shroom3*$^{Gt/Gt}$ mouse embryos. The boxed areas in A and C are magnified in B and D, respectively. (**E-I**) Outlines of individual lens pit cells were traced (dashed white lines) and cell profiles placed on a grid (E,F) to permit quantification of cell width at seven evenly spaced positions (G). Cell height was also quantified (H) and an average cell shape calculated (I). In I, the average cell dimensions are indicated relative to the basal dimension of the control cell. This shows that the *Shroom3*$^{Gt/Gt}$ lens pit cell is shorter and less apically constricted than in the control. (G,H) Error bars are s.e.m.; *, $P<0.05$. (**J**,**K**) Chicken lens pits were electroporated with a GFP- or V5-tagged dominant-negative chicken Shroom3-expressing plasmid. Cryosections were immunofluorescently labeled with phalloidin to visualize F-actin and with GFP or V5 antibodies. Positive cells are outlined (dashed white line). Arrowheads indicate ectopic basal actin. Gray lines between panels indicate that the panels are separated color channels of the same image. (**L**) Quantification of cell width along the apical/basal axis of chicken lens pit cells expressing GFP (gray, control), Shroom3-Flag (blue), DN-cShroom3-V5 (red) or Mena-dn (green). The error bars are s.e.m. The green asterisks indicate a significant difference between Mena-dn and GFP and the red asterisks a significant difference between DN-cShroom-V5 and GFP ($P<0.05$). (**M**) The average shape of cells expressing the indicated transgene is depicted with the relative change in apical and basal cell width. NS, not significant.

(Hildebrand and Soriano, 1999; Nishimura and Takeichi, 2008). To determine whether Shroom3 activity was conserved in the avian lens, we performed electroporations of both the wild-type and a dominant-negative form of Shroom3 in the chick lens pit. Electroporation was performed at stage 11 and the embryos allowed to develop until about stage 19, by which time the lens pit has normally invaginated. Cell shape was analyzed as for the mouse *Shroom3* mutant with the exception that, in conjunction with F-actin labeling, GFP or the epitope-tagged Shroom3 protein was detected with antibodies as a way of defining cell shape. In this experiment, we normalized for cell height and measured cell width over the apical-basal axis.

When a GFP construct was electroporated, GFP-expressing cells were readily detected within the lens pit epithelium (Fig. 3J). Measurements of cell width (Fig. 3L, gray line) indicated that the average cell within the chick lens pit has an apical dimension of ~14 μm and an apical/basal ratio of 0.36 (Fig. 3M, gray). Electroporation of a Shroom3 construct resulted in no significant change in the absolute cell dimensions at either the base or the apex (Fig. 3L) and in an apical/basal ratio of 0.44/0.82=0.53. Thus, for both these controls, lens pit epithelial cells were apically constricted. By contrast, dominant-negative Shroom3 resulted in cells with an apical dimension of ~32 μm. This resulted in an apical/basal ratio of 0.76/0.85=0.91, indicating that the cells had largely failed to apically constrict. Consistent with changes observed in the *Shroom3* mutant mouse lens pit, chick lens pit cells electroporated with the dominant-negative Shroom3 construct frequently showed accumulation of basal actin (Fig. 3K, arrowheads). These data indicate that both the AC and F-actin-recruitment activity of Shroom3 is conserved in avians.

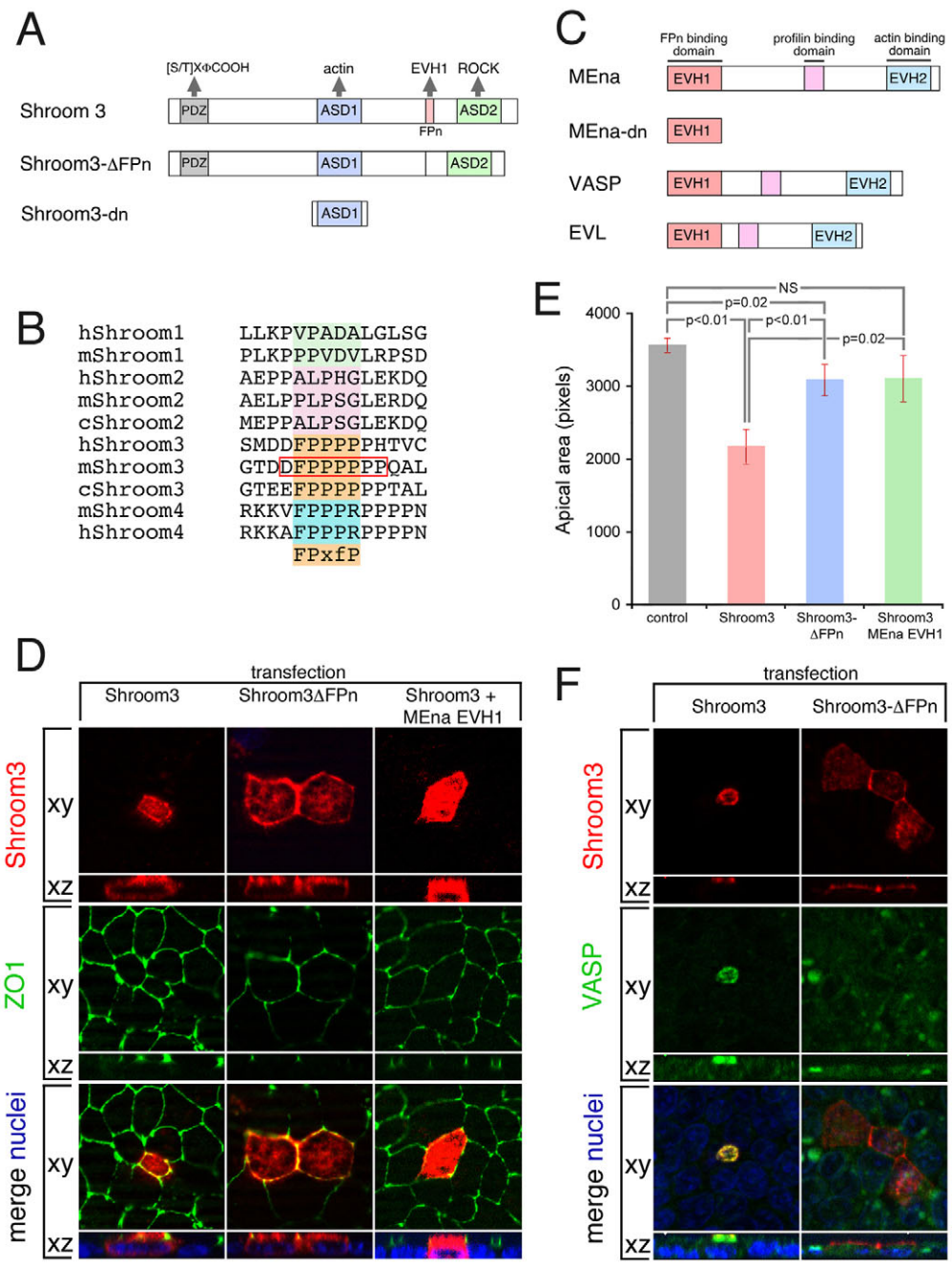

Fig. 4. The FPn domain of Shroom3 is required for apical constriction and apical Vasp localization. (**A**) The wild-type and mutant mouse Shroom3 proteins used. (**B**) Alignment of the amino acid sequences of human (h), mouse (m) and chicken (c) Shroom proteins in the proline-rich (FPn) motif region. The consensus binding site for the Mena/Vasp EVH1 domain is indicated (shaded orange, below the alignment: x, any amino acid; f, hydrophobic amino acid). The red box indicates the amino acids that are deleted in the Shroom3ΔFPn mutant. (**C**) The domain structure of mouse wild-type Mena, dominant-negative Mena (Mena-dn), Vasp and Evl. (**D**) MDCK cells were transiently transfected with the indicated plasmid(s) and immunofluorescently labeled to detect protein expression. Cells were co-labeled with ZO1 to detect apical junctions. Apical structures are detected in the *xy* plane, whereas the apical-basal axis is visualized in the *xz* plane. (**E**) Quantification of the average apical area for cells expressing the indicated proteins. Error bars are s.e.m. (**F**) MDCK cells were transiently transfected with Shroom3-Flag or Shroom3-ΔFPn-Flag and immunofluorescently stained to visualize ectopic Shroom3 and endogenous Vasp. As in D, apical structures are detected in the *xy* plane, whereas the apical-basal axis is visualized in the *xz* plane. Hoechst 33258 labeling was used to visualize nuclei.

The Shroom3 FPn domain mediates apical constriction

Shroom3 is a multi-domain protein that can interact with and/or recruit components of the cytoskeletal machinery, including actin and Rho kinase (Rock1/2) (Hildebrand and Soriano, 1999; Lee et al., 2007; Nishimura and Takeichi, 2008; Taylor et al., 2008). Shroom3 also possesses a proline-rich sequence (FPn) that matches the consensus binding sequence of the Mena/Vasp family of proteins and raises the possibility that there might be an interaction between the FPn-binding (EVH1) domain of Mena/Vasp and Shroom3 (Fig. 4A,C). The biological rationale for this hypothesis is also strong, as Shroom3, Mena and Vasp are all implicated in events of morphogenesis, such as in neural tube closure that requires AC (Hildebrand and Soriano, 1999; Menzies et al., 2004; Kwiatkowski et al., 2007; Roffers-Agarwal et al., 2008).

Among the four mammalian Shroom proteins only Shroom3 can induce AC and, although this activity has been localized to its ASD2 domain, it is clear that additional domains within Shroom3 are also required (Dietz et al., 2006). Amino acid sequence alignment revealed that the FPn domain within Shroom3 perfectly matches the consensus binding sequence of EVH1 domains and is unique among the four mammalian Shroom proteins (Fig. 4B) (Ball et al., 2000; Ball et al., 2002). To determine whether the FPn domain of Shroom3 is required for AC, we transfected wild-type Shroom3 and the FPn deletion mutant into MDCK cells (Fig. 4D). AC activity was assessed by measuring the cell area at the apex and confocal reconstruction of a *z*-axis image revealed the localization of Shroom3 and ZO1, an apical marker (Fig. 4D). Shroom3 induced AC, but the FPn domain deletion mutant showed greatly suppressed activity (Fig. 4D,E).

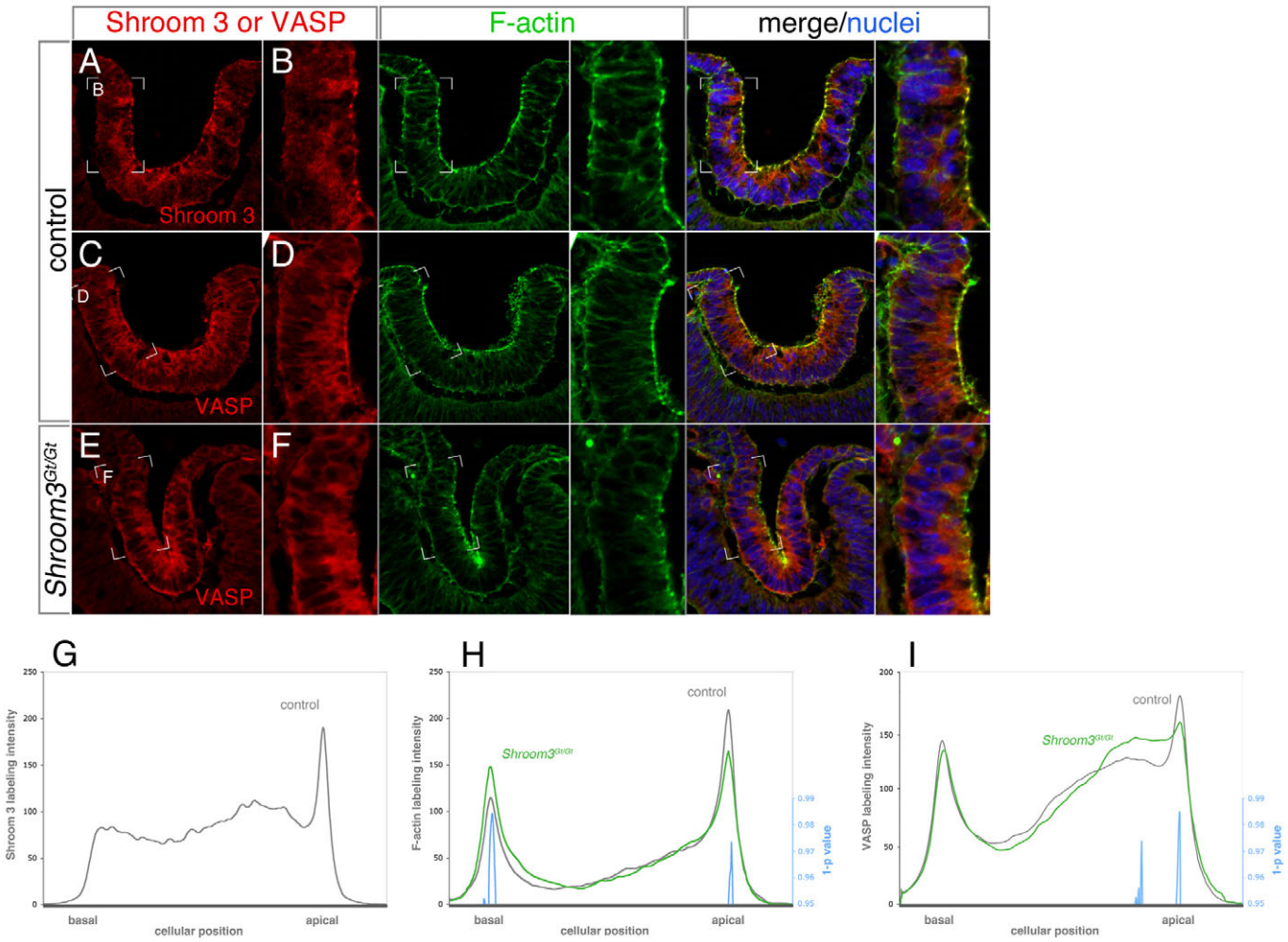

Fig. 5. Apical Vasp localization is reduced in the *Shroom3* mutant lens pit. (**A-F**) Cryosections of control (A-D) and *Shroom3* mutant (E,F) mouse lens pits labeled with phalloidin to visualize F-actin, Hoechst to mark nuclei, and with antibodies specific to Shroom3 or Vasp. The indicated regions of A, C and E are magnified in B, D and F, respectively. Single-channel and merged images are shown in each row. (**G-I**) Quantification of labeling intensity for Shroom3 (G), F-actin (H) and Vasp (I) in control (gray lines) and *Shroom3*$^{Gt/Gt}$ (green lines) lens pit epithelial cells along a basal-to-apical line interval. Statistical significance between the control and mutant was determined for each value along the axis using Student's *t*-test and subtracted from 1. The pixels with values above 0.95 (P<0.05) are indicated by the blue line.

The requirement for the FPn domain implies that an interaction with, or recruitment of, Mena/Vasp might be necessary for AC. To determine whether interfering with Mena/Vasp function can inhibit Shroom3-induced AC, a dominant-negative form of Mena (Mena-dn), consisting of only the EVH1 domain, was co-transfected with Shroom3 into MDCK cells. The EVH1 domain is capable of inhibiting Mena/Vasp function both in vitro and in vivo (Vasioukhin et al., 2000; Eigenthaler et al., 2003). When Mena-dn was co-transfected with wild-type Shroom3, the AC of transfected cells was also suppressed (Fig. 4D,E). To determine whether interfering with Mena/Vasp function in vivo would inhibit AC in the invaginating lens, Mena-dn was electroporated into the prospective lens pits of chicken embryos (Fig. 3L,M). Mena-dn-positive cells had an average apical width of ~37 μm and an average apical/basal ratio of 1.02, which differ significantly from control cells with an average width of ~14 μm and an average apical/basal ratio of 0.36, indicating that these cells failed to undergo AC (Fig. 3L,M).

Apical Vasp accumulation is dependent on Shroom3

The malformed neural tubes of *Shroom3* mutants and of Mena/Vasp-deficient mouse or frog embryos have mislocalized F-actin. Because of this similarity and the dependence of Shroom3 function on the FPn domain, we investigated the possibility that apical Vasp localization is dependent on Shroom3. Immunofluorescent labeling of E10.5 mouse lens pits demonstrated that as with Shroom3 and F-actin (Fig. 5A,B), Vasp is strongly localized to the apex of cells within the lens pit (Fig. 5C,D). Co-staining for Shroom3/F-actin and Vasp/F-actin revealed that the strong immunofluorescent signal of all three is apically co-localized (Fig. 5A-D, merge). When analyzing Vasp immunofluorescent labeling in *Shroom3*$^{Gt/Gt}$ lens pits we observed that the intense apical Vasp signal is consistently reduced or absent (Fig. 5E,F). The levels of Shroom3 (Fig. 5G), F-actin (Fig. 5H) and Vasp (Fig. 5I) labeling throughout the cells of wild-type and *Shroom3*$^{Gt/Gt}$ lens pits were also quantified by analyzing the normalized pixel intensity

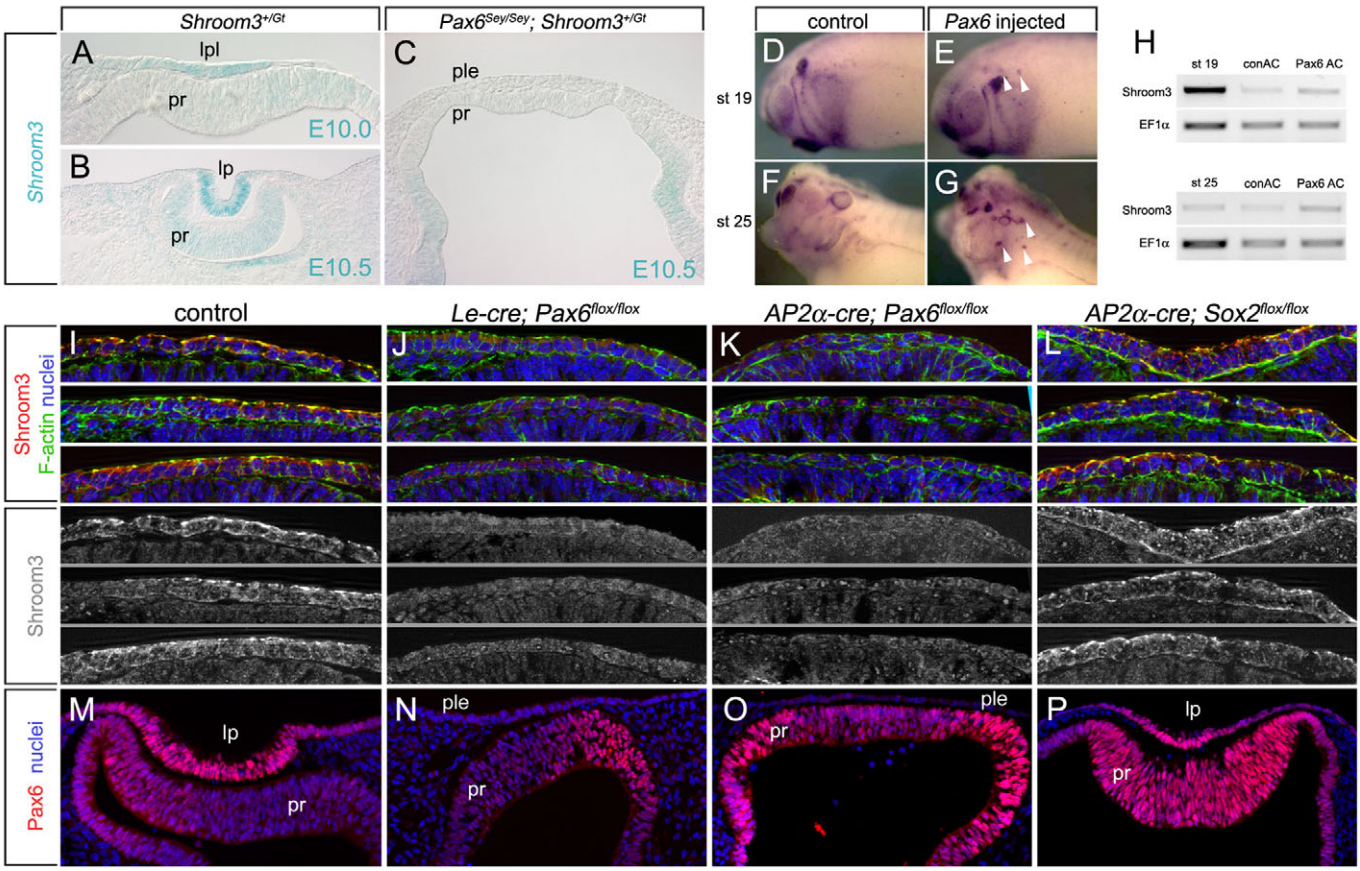

Fig. 6. Pax6 is necessary and sufficient for Shroom3 expression in the lens. (**A-C**) Shroom3 expression from the *lacZ* promoter trap allele was assessed in control (A,B) or *Pax6*$^{Sey/Sey}$ (C) mouse embryos by X-gal staining. (**D-G**) Control or *Pax6* mRNA-injected *Xenopus* embryos were assayed for *Shroom3* expression by in situ hybridization. Arrowheads indicate ectopic *Shroom3* expression. (**H**) RNA was isolated from animal caps derived from control or *Pax6* mRNA-injected *Xenopus* embryos and analyzed by RT-PCR using primers specific to *Xenopus Shroom3* or the housekeeping gene *Ef1α*. (**I-L**) Control mouse embryos (I) or those conditionally deficient for *Pax6* (*Le-Cre; Pax6*$^{flox/flox}$; *AP2α-Cre; Pax6*$^{flox/flox}$) (J,K) or *Sox2* (*AP2α-Cre; Sox2*$^{flox/flox}$) (L) in the surface ectoderm were cryosectioned and labeled for Shroom3. (**M-P**) Pax6 expression in E10.5 wild-type or conditional mutant mouse lens pits as assessed by immunofluorescence. Hoechst 33258 labeling was used to visualize nuclei. lpl, lens placode; ple, presumptive lens ectoderm; lp, lens pit; pr, presumptive retina.

along the apical/basal axis of individual cells within the lens pit. Consistent with our earlier F-actin quantitation (Fig. 2G), we observed a decrease apically and an increase basally in F-actin labeling in *Shroom3*$^{Gt/Gt}$ lens pits (Fig. 5H). On average, the Vasp staining profile was not significantly different basally; however, there was a significant reduction in staining intensity at the apical-most region of the cell, whereas subapically there was a significant increase (Fig. 5I). Similarly, when we assessed the localization of endogenous Vasp protein in MDCK cells, we found that its localization at the cell apex was induced by Shroom3 but was absent when the FPn domain was deleted (Fig. 4F). Together, these data demonstrate that apical Vasp accumulation is dependent on the FPn domain of Shroom3.

Pax6 is necessary and sufficient for Shroom3 expression in the developing lens

The homeodomain transcription factor Pax6 is known to play a crucial role in eye development (Grindley et al., 1995). Pax6 also has an essential cell-autonomous function in the early lens (Fujiwara et al., 1994; Ashery-Padan et al., 2000; Collinson et al., 2000; Smith et al., 2009). One of the features of mouse embryos in which *Pax6* is deleted from the presumptive lens is a complete failure of lens placode invagination (Smith et al., 2009). This raised the possibility that Shroom3 expression might be dependent on Pax6.

To examine this, mice were generated that were heterozygous for the *Shroom3* mutant allele and homozygous for the small eye mutation (*Pax6*$^{Sey/Sey}$). This eliminates functional Pax6 and results in a complete lack of eye development. In contrast to *Shroom3*$^{Gt/+}$ embryos (Fig. 6A,B), X-gal staining of E10.5 *Pax6*$^{Sey/Sey}$; *Shroom3*$^{Gt/+}$ mutant embryos revealed a complete lack of Shroom3 expression in the surface ectoderm where the lens normally invaginates (Fig. 6C). X-gal staining in the optic vesicle (Fig. 6C) showed that Shroom3 dependence on Pax6 is limited to the prospective lens. To ensure that the loss of *Shroom3* expression was not indirectly caused by a lack of Pax6 function in the optic vesicle, mice deficient for Pax6 expression specifically in the surface ectoderm via tissue-specific Cre recombinase-mediated deletion were immunofluorescently labeled for Shroom3. At E9.5, Shroom3 expression is normally first detected apically in surface ectoderm specifically in the region of the lens placode (Fig. 6I). When *Pax6* was deleted from the surface ectoderm using Le-Cre or AP2α-Cre (compare Fig. 6N,O with 6M), lens morphogenesis was inhibited

and Shroom3 expression absent at E9.5 (Fig. 6J,K). By contrast, surface ectodermal deletion of *Sox2*, another transcription factor important for lens development (Smith et al., 2009), did not affect Shroom3 or Pax6 placodal expression (Fig. 6L,P). To determine whether Pax6 is sufficient for Shroom3 expression, *Pax6* mRNA was injected into early *Xenopus* embryos, a procedure that has previously been demonstrated to induce the formation of ectopic eyes and lenses (Altmann et al., 1997; Chow et al., 1999). Embryos were then analyzed for *Shroom3* expression by in situ hybridization (Fig. 6D-G). Control embryos did not produce ectopic lenses and *Shroom3* expression was observed at low levels in the developing eye, otic vesicle, branchial arches (Fig. 6D,F) and in the lens at stage 25 (Fig. 6F). *Pax6*-injected embryos produced regions of intense *Shroom3* expression that were likely to represent ectopic lenses (Fig. 6E,G, arrowheads). The relatively intense in situ labeling of ectopic *Shroom3* compared with that of the endogenous lens might be a consequence of abnormally high transcriptional activation of *Shroom3* and perhaps of differential probe accessibility. RT-PCR analysis of animal caps derived from *Xenopus* embryos injected with control or *Pax6* mRNA also demonstrated an increase in *Shroom3* expression (Fig. 6H). Together, these data demonstrate that Pax6 is both necessary and sufficient for Shroom3 expression in the developing lens.

DISCUSSION

The results presented here indicate that Shroom3 is required for cell shape change within the lens pit during a critical stage of epithelial morphogenesis. The lens pit of *Shroom3* mutant embryos is smaller and misshapen, presumably owing to the reduction in cell height and lack of AC. The *Shroom3* mutant lens pit, in contrast to the wild-type, shows regions of straight epithelium consistent with a complete lack of AC. However, despite this, invagination does occur. Recently, we described a role for filopodia that span the inter-epithelial space between the lens pit and developing retina in coordinating lens pit and optic cup morphogenesis (Chauhan et al., 2009). These filopodia function as physical tethers and actively regulate inter-epithelial distance. In mutants without these filopodia, lens pits are shallow and have a disrupted morphology suggesting that invagination forces are transmitted from the optic cup. Thus, it is likely that the invagination of the lens pit in *Shroom3*$^{Gt/Gt}$ mutants is a consequence of the action of the filopodia that tether presumptive lens and retina. The lens pit bending that does occur in *Shroom3*$^{Gt/Gt}$ mutant embryos might be a result of the abnormal stresses that arise when the absence of AC and the consequent lack of epithelial curvature work in opposition to the action of the filopodia in pulling the lens pit down into the optic cup. Once the appropriate tools become available, it will clearly be of interest to determine whether the absence of filopodia on the *Shroom3*$^{Gt/Gt}$ mutant background results in a flat, non-invaginated lens placode.

The AC activity of Shroom3 is Rho kinase-dependent and is localized within its ASD2 domain, a region that interacts with Rock1/2 (Hildebrand, 2005; Nishimura and Takeichi, 2008). Interfering with the endogenous Shroom3-Rock1/2 interaction disrupts chicken neural tube morphogenesis. However, it is currently unknown whether this interaction is required for lens pit invagination. Shroom3 is apically localized within the lens pit at the onset of invagination, a time and place coincident with Rho kinase activity in apically constricting epithelia. Interestingly, applying a Rho kinase inhibitor to chicken embryos can inhibit lens pit invagination (data not shown), suggesting that Rho kinase activity is required. In addition, RhoA, a Rho GTPase capable of activating Rock1/2, is apically localized within the chicken lens pit (Kinoshita et al., 2008). It is therefore reasonable to speculate that Shroom3 regulates AC in the lens pit in part through its interaction with Rock1/2. The mechanisms by which Rho kinases are activated once recruited by Shroom3 are yet to be determined.

Both F-actin and myosin II are mislocalized in *Shroom3* mutant lens pits, where there is a reduction apically and, frequently, an increase basally. Mislocalization of F-actin and myosin II is also observed in the neural tube of Shroom3-deficient mice and frogs (Hildebrand and Soriano, 1999; Haigo et al., 2003; Hildebrand, 2005). One of the requirements of AC is the presence of an apical F-

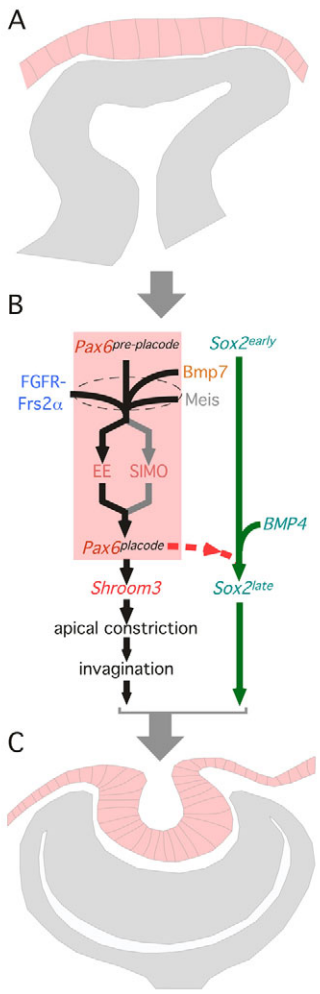

Fig. 7. A model: Pax6-dependent expression of Shroom3 in the lens pit induces apical constriction and facilitates placodal invagination. A model illustrating Shroom3 activity is an important component of the morphogenesis mechanisms required for invagination of the lens pit. (**A**) The activity of Shroom3 becomes important at ~E9.5, just prior to lens pit invagination. (**B**) At this time, inductive signaling that involves Fgf receptor signaling via the Frs2α adapter (blue), Bmp7 signaling (orange) and the Meis transcription factors (gray), results in the transcriptional upregulation of *Pax6* via the EE and SIMO control elements. In turn, Pax6 is required, directly or indirectly, for the expression of *Shroom3* and engagement of the machinery that results in apical constriction in lens pit epithelial cells. (**C**) It is likely that Shroom3-induced apical constriction is one of several mechanisms of morphogenesis that combine to achieve placodal invagination and the formation of a lens pit at E10.5.

actin/myosin network, and disruptions in morphogenesis often accompany mutants that affect this network (Lecuit and Lenne, 2007). It is likely that the mislocalization of F-actin and myosin II in *Shroom3* mutants is partially responsible for the failure of normal AC. Similar to the *Shroom3* mutants, *Mena*/*Vasp* doubly homozygous mutants have neural tube closure defects and an accumulation of basal actin (Menzies et al., 2004). The similarity in phenotypes and the presence of the FPn domain in Shroom3 suggests that the Mena/Vasp proteins are apically recruited by Shroom3 and facilitate the apical accumulation of F-actin in invaginating lens pit cells. Consistent with this idea, Shroom3 is both necessary (Fig. 5) and sufficient (Fig. 4D) for apical Vasp localization. The level of apical Vasp observed in wild-type lens pit cells is significantly reduced in the *Shroom3* mutant. However, subapically there appears to be a trend towards higher levels in the mutant than in the wild type. In the absence of Shroom3, it is possible that the Vasp protein that is normally recruited to the apex now resides in the subapical region of the cell.

Chimeric protein analysis of all four Shroom proteins (Shroom1-4) has demonstrated that the ASD2 domain of each is capable of inducing AC provided that it is linked to the N-terminus of Shroom3. However, the full-length Shroom1, 2 and 4 proteins cannot induce AC themselves, suggesting that a domain within the N-terminus of Shroom3 is also required for AC. We have demonstrated that the proline-rich EVH1 consensus domain within Shroom3 is required for AC (Fig. 4B) and, not surprisingly, the N-terminus region of Shroom3 utilized in the chimeric protein analysis included the proline-rich domain. A stretch of proline residues preceded by a phenylalanine is present in both Shroom3 and Shroom4, but not in Shroom1 and Shroom2. Shroom3 and Shroom4 differ at position 5 in this domain, a position that requires a proline for EVH1 domain binding (Ball et al., 2000; Ball et al., 2002). Because Shroom4 possesses an arginine instead of a proline at this position and Shroom1 and Shroom2 completely lack this domain, it is unlikely that they interact with EVH1 domain-containing proteins. In light of the fact that this domain is required for Shroom3-induced AC, the absence of this domain in other Shroom proteins potentially explains why they cannot induce AC.

Expression analysis revealed that surface ectoderm expression of Shroom3 is restricted to the lens placode at E9.5 (Fig. 6I) and that prior to this stage, expression is not detected (data not shown). This localized expression suggested that Shroom3 might have a role in regulating cell shape and invagination morphogenesis, as we have demonstrated. However, this regional expression also suggested that lens-induction signaling (Lang, 2004) might result in Shroom3 upregulation. This conjecture was confirmed with the observation that various types of Pax6-deficient embryo, including homozygous $Pax6^{Sey}$ (Grindley et al., 1995) and presumptive lens-conditional $Pax6^{flox/flox}$ (Ashery-Padan et al., 2000; Smith et al., 2009) mutants, all failed to upregulate Shroom3. Furthermore, Pax6 gain-of-function experiments in *Xenopus* that are known to produce ectopic lenses (Altmann et al., 1997; Chow et al., 1999) resulted in the ectopic expression of *Shroom3*. These data make a strong case that, directly or indirectly, *Shroom3* expression is Pax6 dependent. This is the first example of a mechanistic link between the inductive signaling and morphogenesis machineries in the lens.

It is also constructive to compare the consequences of *Pax6* and *Sox2* conditional deletion in the presumptive lens. Both of these transcription factors are known to have an important role in the early stages of lens development (Inoue et al., 2007; Smith et al., 2009), but the consequences for lens placode invagination are distinct. When *Pax6* is deleted from the pre-placodal ectoderm, invagination is never observed. By contrast, conditional deletion of *Sox2* results in the formation of a lens pit, albeit shallow. This corresponds very closely to the failure of Shroom3 expression in the *Pax6* mutant and normal Shroom3 expression in the *Sox2* mutant. As discussed above, placodal invagination clearly requires the cooperation of several morphogenesis mechanisms. It will be very interesting to understand which of these, like Shroom3 expression, are dependent on Pax6 and which are dependent on Sox2.

Acknowledgements

We thank Paul Speeg for excellent technical assistance and Dr Frank Gertler for kindly providing the antibody to mouse Vasp. J.B.W. is an early career scientist of the Howard Hughes Medical Institute. We also acknowledge grant support from the NIH to J.B.W. (NIGMS) and R.A.L. (EY15766, EY16241, EY17848, CA131270) and from the Abrahamson Pediatric Eye Institute Endowment at the Children's Hospital Medical Center of Cincinnati to R.A.L. Deposited in PMC for release after 6 months.

Competing interests statement

The authors declare no competing financial interests.

References

Altmann, C. R., Chow, R. L., Lang, R. A. and Hemmati-Brivanlou, A. (1997). Lens induction by Pax-6 in Xenopus laevis. *Dev. Biol.* **185**, 119-123.

Ashery-Padan, R., Marquardt, T., Zhou, X. and Gruss, P. (2000). Pax6 activity in the lens primordium is required for lens formation and for correct placement of a single retina in the eye. *Genes Dev.* **14**, 2701-2711.

Ball, L. J., Kuhne, R., Hoffmann, B., Hafner, A., Schmieder, P., Volkmer-Engert, R., Hof, M., Wahl, M., Schneider-Mergener, J., Walter, U. et al. (2000). Dual epitope recognition by the VASP EVH1 domain modulates polyproline ligand specificity and binding affinity. *EMBO J.* **19**, 4903-4914.

Ball, L. J., Jarchau, T., Oschkinat, H. and Walter, U. (2002). EVH1 domains: structure, function and interactions. *FEBS Lett.* **513**, 45-52.

Barrett, K., Leptin, M. and Settleman, J. (1997). The Rho GTPase and a putative RhoGEF mediate a signaling pathway for the cell shape changes in Drosophila gastrulation. *Cell* **91**, 905-915.

Baum, B. and Perrimon, N. (2001). Spatial control of the actin cytoskeleton in Drosophila epithelial cells. *Nat. Cell Biol.* **3**, 883-890.

Chauhan, B. K., Disanza, A., Choi, S.-Y., Lou, M., Beggs, H. E., Scita, G., Zheng, Y. and Lang, R. A. (2009). Cdc42 and IRSp53-dependent contractile filopodia tether presumptive lens and retina to coordinate epithelial invagination. *Development* **136**, 3657-3667.

Chow, R. L., Altmann, C. R., Lang, R. A. and Hemmati-Brivanlou, A. (1999). Pax6 induces ectopic eyes in a vertebrate. *Development* **126**, 4213-4222.

Collinson, J. M., Hill, R. E. and West, J. D. (2000). Different roles for Pax6 in the optic vesicle and facial epithelium mediate early morphogenesis of the murine eye. *Development* **127**, 945-956.

Dawes-Hoang, R. E., Parmar, K. M., Christiansen, A. E., Phelps, C. B., Brand, A. H. and Wieschaus, E. F. (2005). Folded gastrulation, cell shape change and the control of myosin localization. *Development* **132**, 4165-4178.

Dietz, M. L., Bernaciak, T. M., Vendetti, F., Kielec, J. M. and Hildebrand, J. D. (2006). Differential actin-dependent localization modulates the evolutionarily conserved activity of Shroom family proteins. *J. Biol. Chem.* **281**, 20542-20554.

Eigenthaler, M., Engelhardt, S., Schinke, B., Kobsar, A., Schmitteckert, E., Gambaryan, S., Engelhardt, C. M., Krenn, V., Eliava, M., Jarchau, T. et al. (2003). Disruption of cardiac Ena-VASP protein localization in intercalated disks causes dilated cardiomyopathy. *Am. J. Physiol. Heart Circ. Physiol.* **285**, H2471-H2481.

Fujiwara, M., Uchida, T., Osumi-Yamashita, N. and Eto, K. (1994). Uchida rat (rSey): a new mutant rat with craniofacial abnormalities resembling those of the mouse Sey mutant. *Differentiation* **57**, 31-38.

Gates, J., Mahaffey, J. P., Rogers, S. L., Emerson, M., Rogers, E. M., Sottile, S. L., Van Vactor, D., Gertler, F. B. and Peifer, M. (2007). Enabled plays key roles in embryonic epithelial morphogenesis in Drosophila. *Development* **134**, 2027-2039.

Gates, J., Nowotarski, S. H., Yin, H., Mahaffey, J. P., Bridges, T., Herrera, C., Homem, C. C., Janody, F., Montell, D. J. and Peifer, M. (2009). Enabled and Capping protein play important roles in shaping cell behavior during Drosophila oogenesis. *Dev. Biol.* **333**, 90-107.

Gotoh, N., Ito, M., Yamamoto, S., Yoshino, I., Song, N., Wang, Y., Lax, I., Schlessinger, J., Shibuya, M. and Lang, R. A. (2004). Tyrosine phosphorylation sites on FRS2alpha responsible for Shp2 recruitment are critical for induction of lens and retina. *Proc. Natl. Acad. Sci. USA* **101**, 17144-17149.

Grindley, J. C., Davidson, D. R. and Hill, R. E. (1995). The role of Pax-6 in eye and nasal development. *Development* **121**, 1433-1442.

Hacker, U. and Perrimon, N. (1998). DRhoGEF2 encodes a member of the Dbl family of oncogenes and controls cell shape changes during gastrulation in Drosophila. *Genes Dev.* **12**, 274-284.
Haigo, S. L., Hildebrand, J. D., Harland, R. M. and Wallingford, J. B. (2003). Shroom induces apical constriction and is required for hingepoint formation during neural tube closure. *Curr. Biol.* **13**, 2125-2137.
Hendrix, R. W. and Zwaan, J. (1974). Cell shape regulation and cell cycle in embryonic lens cells. *Nature* **247**, 145-147.
Hendrix, R. W. and Zwaan, J. (1975). The matrix of the optic vesicle-presumptive lens interface during induction of the lens in the chicken embryo. *J. Embryol. Exp. Morphol.* **33**, 1023-1049.
Hildebrand, J. D. (2005). Shroom regulates epithelial cell shape via the apical positioning of an actomyosin network. *J. Cell Sci.* **118**, 5191-5203.
Hildebrand, J. D. and Soriano, P. (1999). Shroom, a PDZ domain-containing actin-binding protein, is required for neural tube morphogenesis in mice. *Cell* **99**, 485-497.
Inoue, M., Kamachi, Y., Matsunami, H., Imada, K., Uchikawa, M. and Kondoh, H. (2007). PAX6 and SOX2-dependent regulation of the Sox2 enhancer N-3 involved in embryonic visual system development. *Genes Cells* **12**, 1049-1061.
Kinoshita, N., Sasai, N., Misaki, K. and Yonemura, S. (2008). Apical accumulation of Rho in the neural plate is important for neural plate cell shape change and neural tube formation. *Mol. Biol. Cell* **19**, 2289-2299.
Kolsch, V., Seher, T., Fernandez-Ballester, G. J., Serrano, L. and Leptin, M. (2007). Control of Drosophila gastrulation by apical localization of adherens junctions and RhoGEF2. *Science* **315**, 384-386.
Krause, M., Dent, E. W., Bear, J. E., Loureiro, J. J. and Gertler, F. B. (2003). Ena/VASP proteins: regulators of the actin cytoskeleton and cell migration. *Annu. Rev. Cell Dev. Biol.* **19**, 541-564.
Kwiatkowski, A. V., Rubinson, D. A., Dent, E. W., Edward van Veen, J., Leslie, J. D., Zhang, J., Mebane, L. M., Philippar, U., Pinheiro, E. M., Burds, A. A. et al. (2007). Ena/VASP Is Required for neuritogenesis in the developing cortex. *Neuron* **56**, 441-455.
Lang, R. A. (2004). Pathways regulating lens induction in the mouse. *Int. J. Dev. Biol.* **48**, 783-791.
Lecuit, T. and Lenne, P. F. (2007). Cell surface mechanics and the control of cell shape, tissue patterns and morphogenesis. *Nat. Rev. Mol. Cell Biol.* **8**, 633-644.
Lee, C., Scherr, H. M. and Wallingford, J. B. (2007). Shroom family proteins regulate gamma-tubulin distribution and microtubule architecture during epithelial cell shape change. *Development* **134**, 1431-1441.
Lee, C., Le, M. P. and Wallingford, J. B. (2009). The shroom family proteins play broad roles in the morphogenesis of thickened epithelial sheets. *Dev. Dyn.* **238**, 1480-1491.
Lee, J. Y. and Harland, R. M. (2007). Actomyosin contractility and microtubules drive apical constriction in Xenopus bottle cells. *Dev. Biol.* **311**, 40-52.
Menzies, A. S., Aszodi, A., Williams, S. E., Pfeifer, A., Wehman, A. M., Goh, K. L., Mason, C. A., Fassler, R. and Gertler, F. B. (2004). Mena and vasodilator-stimulated phosphoprotein are required for multiple actin-dependent processes that shape the vertebrate nervous system. *J. Neurosci.* **24**, 8029-8038.
Nikolaidou, K. K. and Barrett, K. (2004). A Rho GTPase signaling pathway is used reiteratively in epithelial folding and potentially selects the outcome of Rho activation. *Curr. Biol.* **14**, 1822-1826.
Nishimura, T. and Takeichi, M. (2008). Shroom3-mediated recruitment of Rho kinases to the apical cell junctions regulates epithelial and neuroepithelial planar remodeling. *Development* **135**, 1493-1502.
Roffers-Agarwal, J., Xanthos, J. B., Kragtorp, K. A. and Miller, J. R. (2008). Enabled (Xena) regulates neural plate morphogenesis, apical constriction, and cellular adhesion required for neural tube closure in Xenopus. *Dev. Biol.* **314**, 393-403.
Smith, A. N., Miller, L. A., Song, N., Taketo, M. M. and Lang, R. A. (2005). The duality of beta-catenin function: a requirement in lens morphogenesis and signaling suppression of lens fate in periocular ectoderm. *Dev. Biol.* **285**, 477-489.
Smith, A. N., Miller, L.-A., Radice, G., Ashery-Padan, R. and Lang, R. A. (2009). Stage-dependent modes of Pax6-Sox2 epistasis regulate lens development and eye morphogenesis. *Development* **136**, 2977-2985.
Taylor, J., Chung, K. H., Figueroa, C., Zurawski, J., Dickson, H. M., Brace, E. J., Avery, A. W., Turner, D. L. and Vojtek, A. B. (2008). The scaffold protein POSH regulates axon outgrowth. *Mol. Biol. Cell* **19**, 5181-5192.
Vasioukhin, V., Bauer, C., Yin, M. and Fuchs, E. (2000). Directed actin polymerization is the driving force for epithelial cell-cell adhesion. *Cell* **100**, 209-219.
Wawersik, S., Purcell, P., Rauchman, M., Dudley, A. T., Robertson, E. J. and Maas, R. (1999). BMP7 acts in murine lens placode development. *Dev. Biol.* **207**, 176-188.